Immunoprecipitation of Nonerythrocyte Spectrin Within Live Cells following Microinjection of Specific Antibodies: Relation to Cytoskeletal Structures

PAUL H. MANGEAT and KEITH BURRIDGE
Laboratories of Cell Biology, Department of Anatomy, University of North Carolina, Chapel Hill, North Carolina 27514

ABSTRACT The intracellular precipitation of nonerythrocyte spectrin has been achieved by the microinjection into cells of either a monoclonal antibody (IgM) directed against the α chain of nonerythrocyte spectrin or an affinity-purified polyclonal antibody raised against bovine brain spectrin (fodrin). This antibody-induced precipitation of spectrin was observed in fibroblastic and epithelial cell types, including embryonic bovine tracheal fibroblasts, a bovine kidney epithelial cell line (MDBK), Hela cells, gerbil fibroma cells, and fibroblast lines of human and mouse origins. The precipitation of the spectrin was specific and two proteins with a similar distribution to the nonerythrocyte spectrin were not induced to co-precipitate in the spectrin aggregates. Comparing the two types of antibody microinjected, the affinity-purified polyclonal antibody resulted in more compact aggregates of spectrin and these were more frequently aligned with microfilament bundles. The rate at which the spectrin aggregates were cleared into presumptive lysosomes varied with different cell types: in some such as the bovine kidney epithelial cells, this appeared complete within 3 h after microinjection, whereas in some of the fibroblasts the spectrin aggregates were prominent in the cytoplasm at 24 and even 48 h after microinjection. Microfilament bundles appeared unaffected by the aggregation of spectrin. We conclude that the integrity of the actin microfilament bundles does not require nonerythrocyte spectrin and that most probably these structures are linked at their termini to the membrane through proteins other than nonerythrocyte spectrin. No effect of the intracellular spectrin precipitation was observed on cell shape, or on the distribution of coated vesicles or microtubules. The aggregation of the nonerythrocyte spectrin, however, did affect the distribution of the vimentin type of intermediate filaments in most of the cell types studied. These filaments became more distorted and condensed, but generally did not collapse around the nucleus as occurs following microtubule disruption induced by colchicine treatment. The clumped intermediate filaments were frequently seen to coincide with regions of aggregated spectrin. This aggregation of intermediate filaments was not induced by microinjection of irrelevant antibodies, nor was it induced by the monoclonal antibody against spectrin in cells with which it did not cross-react. We suggest that there may exist some association (either direct or indirect) between the vimentin type of intermediate filaments and nonerythrocyte spectrin, and that possibly the nonerythrocyte spectrin is involved in linking intermediate filaments to the plasma membrane. Finally, in contrast to the situation in erythrocytes, our data do not support a major role for a nonerythrocyte spectrin network as the structural basis of cytoskeletal organization underlying the plasma membrane in fibroblasts. Instead, nonerythrocyte spectrin appears to be just one element in a far more complex submembranous meshwork than that found in erythrocytes.

THE JOURNAL OF CELL BIOLOGY · VOLUME 98 APRIL 1984 1363–1377

Since the first report of the presence of immunologically cross-reactive material to erythrocyte spectrin in nonerythroid tissue (18), convergent data from different laboratories have emphasized the presence of a family of proteins related to erythrocyte spectrin structurally, immunologically, and functionally in essentially every nonerythroid tissue and cell-type examined (2, 6, 12, 13, 24, 37, 40). These proteins, referred to here as nonerythrocyte spectrins, are composed of a high molecular weight polypeptide doublet and consist in solution of the tetramer $\alpha 2\beta 2$, with a flexible rod-shaped morphology when analyzed by platinum rotary shadowing (2, 12, 14, 24). In the brain the protein has been identified (2, 6, 12–14) as that previously called fodrin (31) or CBPI for calmodulin-binding protein (7) or calspectin (24). In the brush border of intestinal epithelium Glenney et al. (12) have documented the presence of a similar protein specifically distributed in the terminal web of the brush border and termed TW260/240. By indirect immunofluorescence microscopy of cross-sections from different tissues and cells, the erythrocyte spectrin molecules have been found in a submembranous localization and by analogy with erythrocyte spectrin are believed to form a subcortical meshwork within the cell (12, 31, 40). At the electron microscopic level this network has been visualized in the brush border of the intestinal epithelium by Hirokawa et al. (22) using the quick-freeze, deep-etch, platinum replica technique.

Although structural and immunological similarities between nonerythrocyte and erythrocyte spectrins are now well documented (2, 6, 12–14, 18, 24, 37, 40) the function of the nonerythrocyte spectrin has not been established. We do know, however, that nonerythrocyte spectrin binds F-actin (2, 6, 7, 12, 24, 31, 41) and calmodulin (7, 12, 24), binds to inverted erythrocyte membranes depleted of spectrin and actin (2, 6), competes in this binding with erythrocyte spectrin (2, 6), and certainly in the case of brain spectrin, possesses an ankyrin binding site (6).

One approach to determining the function of nonerythrocyte spectrin has been to develop a homogeneous model system in which it is possible to perform reassociation experiments similar to those that have led to our understanding of how proteins of the erythrocyte cytoskeleton associate with the erythrocyte membrane. Towards developing such a system we have purified Hela cell spectrin and shown selective binding to a specific membrane fraction from the same Hela cells (35), but the binding site has still to be identified.

In this paper we have begun another approach towards determining the function of the nonerythrocyte spectrin by microinjecting specific antibodies against spectrin into live cells. Both monoclonal (IgM) and high-titer, affinity-purified polyclonal antibodies against nonerythrocyte spectrin result in the quantitative and selective precipitation of these spectrin molecules within the injected cells. This intracellular immunoprecipitation of nonerythrocyte spectrin induced no alteration in the distribution of the actin microfilament bundles, the microtubules, or the coated vesicles; nor was the cell shape affected. However, following this microinjection, the organization of the vimentin type of intermediate filaments was affected such that the intermediate filaments in many of the injected cells were more condensed than normal and these condensed regions frequently coincided with the aggregates of precipitated spectrin.

MATERIALS AND METHODS

Cell Culture: The cells used in the present study were embryonic bovine tracheal cells (NBL-4) obtained from the American Type Culture collection (CCL44) and referred to here as EBTr[1], a human fibroblast line BG-9 obtained from Dr. Ken Jacobson (Chapel Hill), a gerbil fibroma (ATCC CCL146), Madin-Darby bovine kidney (MDBK) epithelial cells (ATCC CCL22), and Hela cells. Cells were grown in Dulbecco's modified Eagle's medium (DME) containing either 2 or 10% fetal calf serum and supplemented with 100 U/ml penicillin and 100 μg/ml streptomycin. Cells were microinjected or treated for indirect immunofluorescence 1–3 d after plating. Cells were incubated with 1 or 10 μM colcemid in Dulbecco's modified Eagle's medium 10% fetal calf serum 1 d after being seeded on glass coverslips. Total cell lysates from EBTr or BG-9 cell lines were obtained by scraping a 6-cm confluent Petri dish in 120 μl of 1:1 diluted gel electrophoresis sample buffer (29).

Isolation of Monoclonal Antibodies: Hybridoma clone PHM61 has been isolated from a fusion of myeloma cells (NS1) with spleen cells of mice immunized with pig brain spectrin, according to the original method of Köhler and Milstein (28) except fusion was mediated by polyethyleneglycol described in detail by Kennett (26). Screening of the resulting hybridomas has been performed by indirect immunofluorescence on EBTr cells. For microinjection, 200 ml of culture medium of hybridoma PHM61 were fractionated by the addition of ammonium sulfate to 50% saturation followed by dialysis against phosphate buffer saline (PBS) and another precipitation at 40% saturation of ammonium sulfate. The final pellet was dissolved in ~2 ml of injection buffer containing 10 mM potassium phosphate pH 7.2 and 75 mM potassium chloride and dialyzed extensively against the same buffer with two changes. The antibody was then fractionated in 20-μl aliquots and stored until use at −80°C. High titer ascites fluids were also obtained from hybridoma-bearing mice. These were not found satisfactory for microinjection experiments because of the presence of significant amounts of normal mouse antibodies, unrelated to the hybridoma.

A second monoclonal antibody, PHM526, was also used in these studies. This antibody did not cross-react with nonerythrocyte spectrins but it gave an immunofluorescent staining pattern on cells that was very similar to antibodies against nonerythrocyte spectrin. The cross-reactive antigen has not yet been identified but the antibody was obtained unexpectedly during the development of monoclonal antibodies against coated vesicles (P. Mangeat, unpublished results).

Affinity Purification of Rabbit Antibovine Brain Spectrin Antibody: Rabbit anti-bovine brain spectrin antibody characterized previously (6) has been affinity purified by two different procedures. In one procedure 7.5% polyacrylamide-SDS preparative gels were run with purified pig brain spectrin and stained with Coomassie Blue. Portions of the gels containing the protein were cut out, destained, and homogenized in Tris-buffered saline (TBS) (50 mM Tris-HCl pH 7.6, 150 mM NaCl, 0.1% NaN_3). The homogenized gel was used batch-wise as an affinity matrix to purify the specific antibodies from total serum. The affinity purified antibodies were eluted by incubating the gel twice with 0.1 M glycine-HCl pH 2.3. In the second procedure purified pig brain spectrin was coupled onto ultrogel ACA22 (LKB) that had been activated with glutaraldehyde (42). Serum was passed through the affinity matrix and then washed with TBS until no protein was detected eluting from the column. Bound antibody was eluted with 0.1 M glycine-HCl, pH 2.3. The eluted material from either procedure was immediately neutralized with 1 M Tris base. For indirect immunofluorescence the antibodies were concentrated and stored in aliquots in TBS containing ~5 mg/ml BSA at −20°C. For microinjection the eluted affinity-purified antibodies were concentrated by dialyzing against 70% sucrose in PBS, then dialyzed extensively against injection buffer and kept on ice. For microinjection the antibodies were used at ~1.5 mg/ml, a concentration equivalent to 100 times the concentration that is needed to generate bright fluorescence in indirect immunofluorescence.

Microinjection: The techniques of Graessmann and Graessmann (21) were used to inject the proteins mechanically into living cells. Briefly, cells growing on glass coverslips (12-mm diam) were microinjected with the aid of a glass capillary. The capillary consists of 0.7–1.0 mm borosilicate glass tubing (Arthur Thomas Co., Philadelphia, PA) prepulled manually over a flame, then pulled automatically (5.4–5.6 Amp) on a workshop-made needle puller. The tip of the capillary (1–2-μm diam) was controlled under a Leitz diavert microscope and attached to a Leitz micromanipulator equipped with a pressure and suction device.

Indirect Immunofluorescence Microscopy and Antibodies: For indirect double-label immunofluorescence, EBTr cells on glass coverslips were washed briefly in PBS, fixed with 3.7% formaldehyde in PBS (5–15 min), and permeabilized with 0.1% Triton X-100 in TBS (4 min at room temperature). After being rinsed in TBS, the coverslips were incubated generally for 30 min at 37°C with the first antibodies, but 90 min at 37°C in the case of the PHM61 monoclonal antibody. The different antibodies used were: ~10 μg/

[1] *Abbreviations used in this paper*: EBTr, embryonic bovine tracheal cells; FITC (RITC), fluorescein (rhodamine) isothiocyanate; MDBK, Madin-Darby bovine kidney; TBS, Tris-buffered saline.

ml of affinity-purified rabbit anti-bovine brain spectrin antibody; monoclonal antibody PHM61 (ascites fluid at 1:250–1:500 dilution); guinea pig antitubulin antibodies (serum at 1:50 dilution) (3); rabbit anticoated vesicles (serum at 1:100 dilution) prepared by repeated injection of pig brain clathrin as described by Keen et al. (25); rabbit autoimmune anti-intermediate filaments (serum at 1:50 dilution) (19); mouse monoclonal antibody JLB7 anti-intermediate filaments (ascites fluid at 1:70 dilution) (33); monoclonal antibody PHM526 (ascites fluid 1:25 dilution); rabbit anti-36-kd protein (serum at 1:80 dilution) (39). Actin microfilament bundles were stained with 7-nitrobenz-2-oxa-1, 3-diazole (NBD)-phallicidin (0.3 U, Molecular Probes, Inc., Junction City, OR) (1). After incubation with the first antibodies, the cells were washed and incubated 30 min at 37°C with appropriate fluorescein- or rhodamine-conjugated second antibodies obtained from Cappel Laboratories (Cochranville, PA) and used at dilutions of 1:25–1:50. These were fluorescein or rhodamine isothiocyanate (FITC or RITC)-labeled goat anti-rabbit IgG (heavy and light chains), FITC- or RITC-labeled goat anti-mouse IgG (heavy and light chains), FITC-labeled goat anti-guinea pig IgG (heavy and light chains). After extensive washing in TBS, the coverslips were mounted on microscope slides in a drop of gelvatol (Monsanto Co., St. Louis, MO) containing *N*-propylgallate to reduce photobleaching (11). The cells were observed on a Leitz Orthoplan epifluorescence photomicroscope equipped with a Zeiss plan Apo 63 × oil phase lens. Fluorescence micrographs were recorded on Kodak Tri-X film and phase contrast micrographs were recorded on either Kodak Tri-X or Technical pan film.

Preparation of Cytoskeletons: Detergent insoluble cytoskeletons were prepared as follows: cells were washed twice in PBS and once at room temperature in extraction buffer (10 mM HEPES pH 7.4, 0.3 M sucrose, 50 mM NaCl, 2.5 mM $MgCl_2$, 2 mM phenylmethylsulfonyl fluoride) without added Triton X-100. The cells were then incubated for 2 min on ice with ice-cold extraction buffer containing 0.5% Triton X-100. Cells were washed once with extraction buffer without Triton X-100 at room temperature followed by one wash in PBS. The cells were then fixed for 30 min with 3.7% formaldehyde in PBS and subsequently processed for indirect immunofluorescence.

SDS-gel Electrophoresis and Immunoblotting: SDS-PAGE was performed in slab gels according to the method of Laemmli (29). 7.5% polyacrylamide gels contained 0.19% bisacrylamide. For immunoblotting, the method of Towbin et al. (43) was used slightly modified. After a 3-h electrophoretic transfer at 0.5 Amp onto nitrocellulose paper (Millipore Co., Bedford, MA), the nitrocellulose strips were washed 1 h in 3% BSA, 0.25% gelatin in TBS, then incubated 2 h at room temperature with a culture medium supernatant solution from PHM61 hybridoma containing 0.25% gelatin and 1% hemoglobin. After extensive washing of the nitrocellulose strips first in 0.25% gelatin in TBS, then in TBS, the strips were incubated 1 h at room temperature with ^{125}I-affinity-purified goat anti-mouse IgG (heavy and light chains) obtained from Cappel Laboratories and iodinated by the chloramine T method (23) using iodine-125 (New England Nuclear, Boston, MA) as described previously (6) but keeping the IgG solution in PBS. The iodinated second antibody was used with a specific activity of ~5 × 10^6 cpm/μg IgG. Nitrocellulose strips were incubated with a solution containing ~4 × 10^6 cpm/ml and 2% hemoglobin in TBS, washed, air-dried, and autoradiographed at −80°C on Kodak X-Omat AR film using an intensifying screen (8–12 h, Fig. 1, *b–d*; 48 h, Fig. 1 *e*). In the case of the characterization of the affinity-purified polyclonal anti-brain spectrin antibody (Fig. 1*e*), iodinated affinity-purified goat anti-rabbit IgG (heavy and light chains) was used as second antibody at ~10^5 cpm/ml.

Purification of Proteins: Human erythrocyte spectrin and pig brain spectrin were purified as described previously (6). Separation of α and β chains of pig brain spectrin was performed by cutting out each band that had been separated by SDS-PAGE (with a four times longer running time). Each chain was then recovered by electroelution from the pieces of gels and dialyzed against 0.125 M Tris-HCl pH 6.8 containing 0.1% β mercaptoethanol. Vinculin was purified according to Feramisco and Burridge (8) and conjugated with RITC instead of FITC as initially reported by Burridge and Feramisco (5). The RITC-labeled vinculin was then concentrated against 70% sucrose in PBS and extensively dialyzed against injection buffer and kept on ice. The rhodamine-labeled goat anti-mouse IgG antibody (Cappel Laboratories) used in the injection experiments was used at 2 mg/ml after extensive dialysis against the injection buffer.

RESULTS

Characterization of Monoclonal Antibody PHM61

In our studies of nonerythrocyte spectrin we have begun to develop a series of monoclonal antibodies against the protein. One of these monoclonal antibodies (PHM61) has proved to be most useful in microinjection studies and will be described here in more detail. Immunoblot analysis of PHM61 has been performed on electrophoretic transfers of purified pig brain spectrin, human erythrocyte spectrin, and total lysates of EBTr and BG-9 cells. As shown in Fig. 1, *a* and *b*, the antibody binds specifically to the brain protein (lane *1*), as well as to a lower molecular weight degradation product of the protein (6, 35) and to a band of similar molecular weight in the gels of both the bovine (lane *3*) and human (lane *4*) cell lines. No cross-reactivity is seen with human erythrocyte spectrin (lane *2*). Applying this analysis to the separated α and β chains of

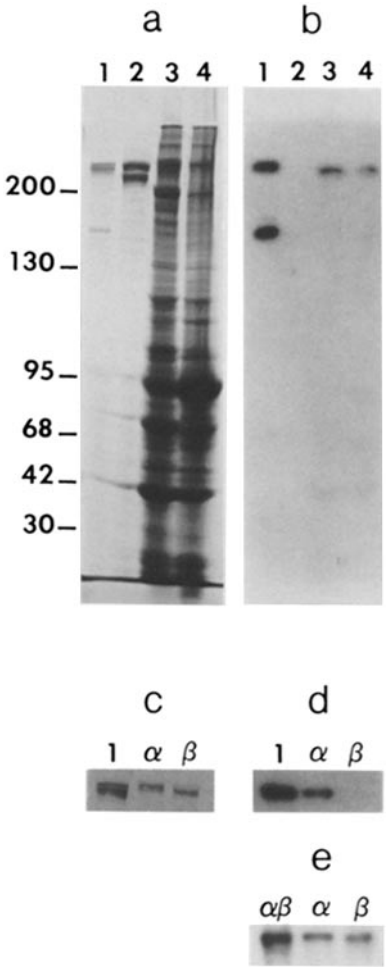

FIGURE 1 Characterization of the anti-pig brain spectrin monoclonal antibody PHM61 and of the affinity-purified polyclonal anti-brain spectrin antibody used in microinjection experiments. (*a* and *c*) Coomassie Blue staining of a 7.5% polyacrylamide SDS gel. Lane *1*, pig brain spectrin; lane *2*, human erythrocyte spectrin; lane *3*, total EBTr cell lysate; lane *4*, total BG-9 cell lysate; lane α, α chain of pig brain spectrin; lane β, β chain of pig brain spectrin. (*b* and *d*) Autoradiographs of immunoblots of replicas of the same gels shown in a and c, stained first with monoclonal antibody PHM61 followed by ^{125}I-goat anti-mouse IgG. It should be noted that a proteolytic fragment of the α chain of brain spectrin transferred to the nitrocellulose with a much higher efficiency than the intact α and β chains, and hence is disproportionately prominent in the autoradiograph. (e) Autoradiograph of immunoblot of a similar gel as in *b* where instead of pig brain spectrin (lane *1*) a mixture of α and β chains (lane αβ) was electrophoresed. The total amount of α and β chains used was half the amount used in c and *d*. The nitrocellulose strip was stained first with a 1:100 dilution of the affinity-purified polyclonal antibody used in microinjection experiments followed by ^{125}I-goat anti-rabbit IgG.

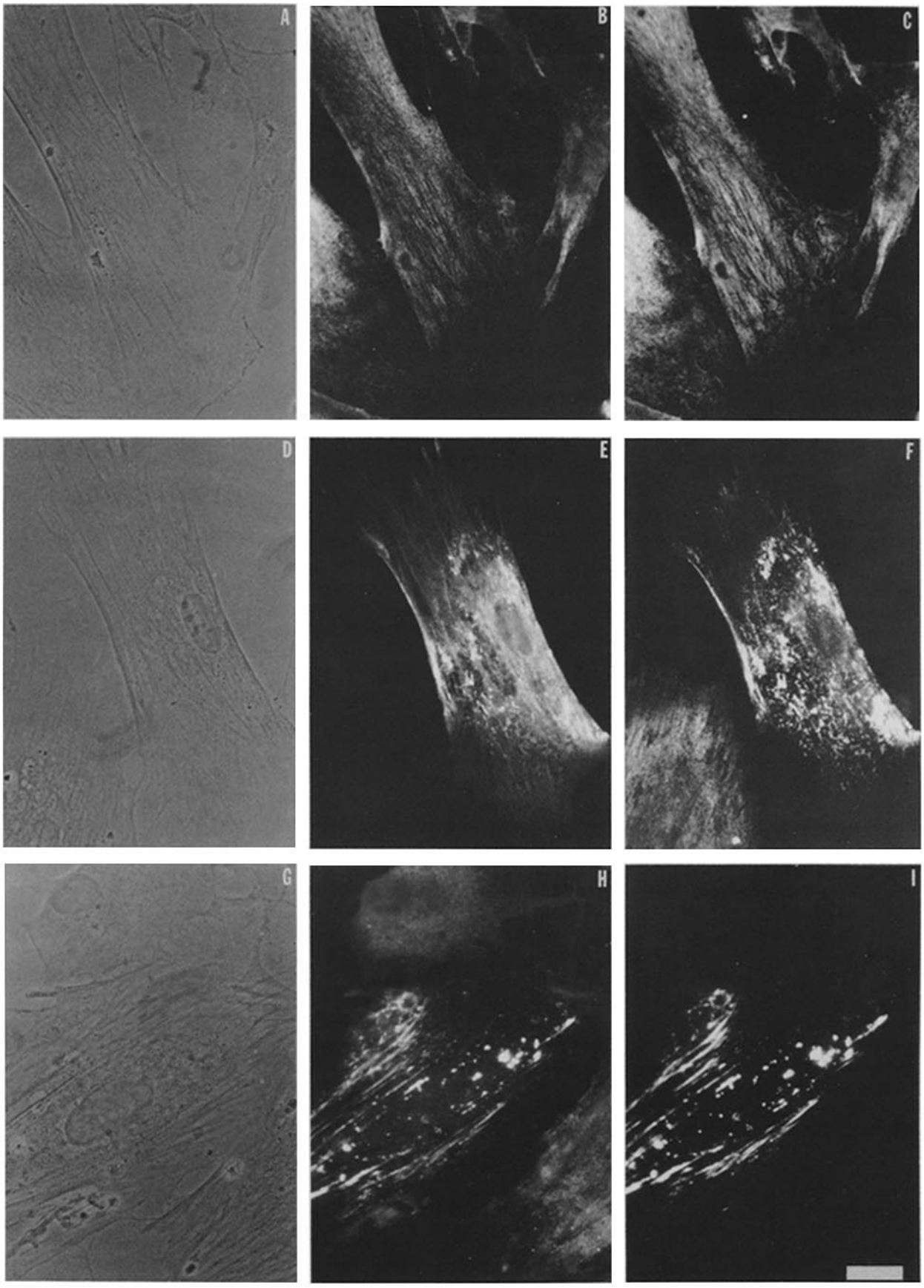
A
B
C
D
E
F
G
H
I

pig brain spectrin, only the α chain is recognized by the antibody (Fig. 1, *c* and *d*). We conclude that PHM61 is specific for the α chain of nonerythrocyte spectrin from porcine, bovine, and human origin.

PHM61 is an IgM molecule (data not shown). When it is used for indirect immunofluorescence on cultured cells a typical diffuse, mottled pattern characteristic of nonerythrocyte spectrin is seen (Fig. 2 *B*). An indistinguishable pattern is obtained when the same cells are stained simultaneously with characterized (reference 6 and Fig. 1 *e*) rabbit anti-bovine brain spectrin antibody (Fig. 2 *C*).

Microinjection of Nonerythrocyte Spectrin Antibodies into Embryonic Bovine Tracheal Fibroblasts

We have microinjected into living EBTr cells either PHM61 (Fig. 2 *E*) or an affinity-purified rabbit anti-bovine brain spectrin antibody (Fig. 2 *I*) and have examined the distribution of spectrin in the injected cells by counterstaining the same cells either with the affinity-purified rabbit antibody (Fig. 2 *F*) or with the monoclonal, PHM61 (Fig. 2 *H*). Upon microinjection into cells both antibodies altered drastically the distribution of the spectrin. Compared with the normal localization of the protein (Fig. 2, *B–C*), the spectrin in the cells injected with PHM61 was aggregated into large patches. These aggregates were generally randomly distributed within the cell, but some faint staining along stress fibers was often apparent (Fig. 2 *E*; see also Figs. 5, *A* and *C* and 6 *C*). On the other hand, the spectrin in cells microinjected with the affinity-purified rabbit antibody was more aggregated within the cell and frequently small aggregates could be seen to align with the cell's stress fibers (Figs. 2 *I*, 5 *E*, 10, *E* and *H*).

We wanted to be sure that all the spectrin was being precipitated into these aggregates following microinjection of the affinity-purified rabbit antibody. Since PHM61 is only specific for the α chain of nonerythrocyte spectrin (see above), counterstaining with this antibody would not indicate whether all the β chain had also precipitated. Not having a specific β chain antibody, we decided to counterstain the injected cells with the same rabbit polyclonal antibody that is known to react equally with both chains (Fig. 1 *E*). So that we would know unambiguously which cells had been microinjected with this antibody we co-microinjected rhodamine-conjugated vinculin together with this affinity-purified antibody. The rhodamine-conjugated vinculin incorporated into the adhesion plaques (5) and enabled easy detection of the injected cells (Fig. 3 *A*). Counterstaining the injected cells with the rabbit anti-bovine brain spectrin clearly indicated that all the spectrin was in the aggregates (Fig. 3 *B*). Assuming that we can detect all the cell's spectrin by indirect immunofluorescence microscopy, this would indicate that all the spectrin in the cell had been bound by the microinjected antibody. It was possible that the microinjected antibodies were affecting only a cytoplasmic pool of spectrin and that spectrin that was associated with the plasma membrane or the cytoskeleton was not being precipitated. To pursue this possibility further, cells that had been injected with antispectrin were subsequently permeabilized with 0.5% Triton X-100 before fixation. Immunofluorescent analysis of such Triton X-100-insoluble cytoskeletons revealed the aggregated spectrin still associated with the cytoskeleton. By comparison with cells that had not been injected, it was clear that spectrin that had previously been associated diffusely with the cytoskeleton had been concentrated into these compact aggregates (Fig. 3, *C–D*).

We have investigated whether this antibody-induced precipitation of spectrin within cells also caused proteins with a similar distribution to be clustered into these aggregates. Two antibodies that gave similar staining patterns to antispectrin but that did not cross-react with spectrin were used in this study. One of these was an antibody against a 36-kd protein, which is a major substrate for $pp60^{src}$ kinase (20, 38, 39) and the other was a monoclonal antibody (PHM 526) against an as yet undetermined antigen. As shown in Fig. 4, the antibody-induced aggregation of spectrin within cells did not result in a concomitant aggregation of these other proteins.

Effect of Microinjection of Nonerythrocyte Spectrin Antibodies on Cytoskeletal Structures

Because of its structural similarities to erythrocyte spectrin and because of its submembranous location in cells, nonerythrocyte spectrin has been suggested to have equivalent functions to the erythrocyte protein, in particular to be involved in mediating the attachment of cytoskeletal elements to the membrane. Since we could cause the spectrin in nonerythrocytes to precipitate into aggregates by microinjecting specific antibodies into cells we wanted to determine how this might affect other cytoskeletal structures in the same cells. We have, therefore, examined the distribution of microtubules (Fig. 5 *B*), coated vesicles (Fig. 5 *D*), microfilaments (Fig. 5 *F*), and the vimentin class of intermediate filaments (Fig. 5 *H*) in EBTr cells that were microinjected with nonerythrocyte spectrin antibodies. Whether the cells were injected with the monoclonal or affinity-purified polyclonal antibody and regardless of the time after injection at which the cells were examined, no effect of the spectrin precipitation was observed on the distribution of microtubules, coated vesicles, or microfilament bundles. Similarly the injected cells were not observed to change shape significantly. On the other hand the majority of injected cells (75%) revealed distorted vimentin intermediate filaments (Fig. 5 *H*). This effect on the vimentin filaments was not due to a mechanical artifact of the microinjection procedure as was seen in a time-course study. The distribution of vimentin filaments remained normal immediately after the injection of the antibody (5–20 min) and so

FIGURE 2 Indirect double-label immunofluorescence characterization of nonerythrocyte spectrin in uninjected and microinjected EBTr cells. (*A–C*) Control uninjected cells; (*D–F*), cell microinjected with mouse monoclonal antibody PHM61 3 h before fixation; (*G–I*) cell microinjected with affinity-purified rabbit anti-bovine brain spectrin 5 h before fixation. After fixation and permeabilization cells were reacted with either mouse monoclonal antibody PHM61 (*B* and *H*) or affinity-purified rabbit anti-bovine brain spectrin (*C* and *F*). Rhodamine-conjugated goat anti-rabbit IgG and fluorescein-conjugated goat anti-mouse IgG antibodies were used as second antibodies. (*A*, *D*, and *G*) Phase contrast micrographs; (*B*, *E*, and *H*) the same fields selectively viewed for fluorescein fluorescence to allow the monoclonal antibody to be visualized, (*C*, *F*, and *I*) the same fields selectively viewed for rhodamine fluorescence to allow the distribution of affinity purified rabbit anti-bovine brain spectrin to be visualized. Bar, 30 μm.

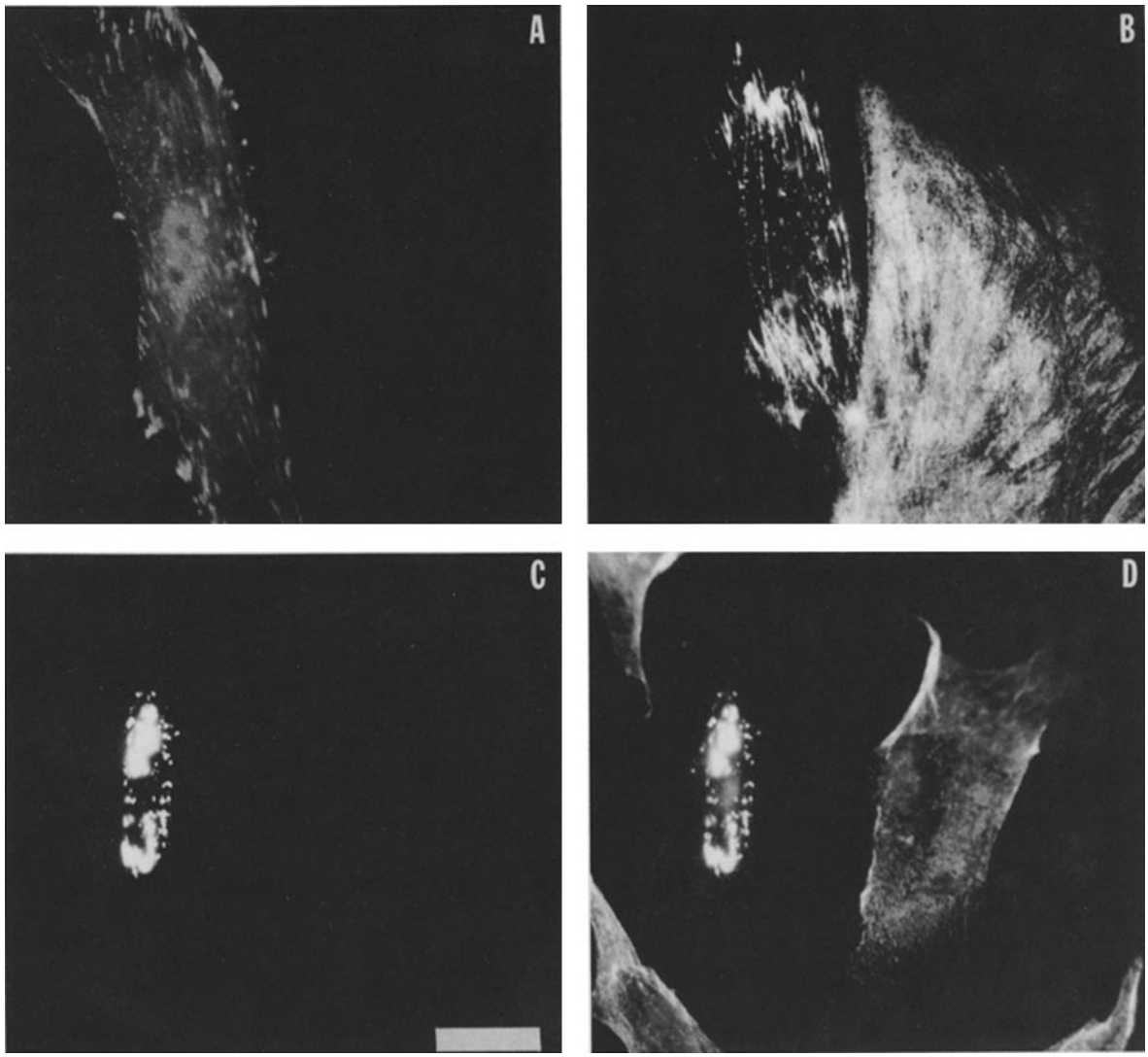

FIGURE 3 Quantitative precipitation of EBTr cell spectrin following microinjection of affinity-purified anti-brain spectrin antibody. (*A* and *B*) Co-microinjection of an EBTr cell with rhodamine-conjugated vinculin and brain spectrin antibody. 3 h after microinjection the cells were fixed, permeabilized, and stained with the affinity-purified rabbit anti-brain spectrin antibody, followed by a second fluorescein-labeled antibody directed against the first. In *A* the cells were viewed with rhodamine-specific optics to visualize the vinculin (and hence the injected cell) and in *B* the cells have been visualized with fluorescein-specific optics to visualize the spectrin distribution. Note the comparison of the spectrin distribution between the injected and uninjected cells. In *C* and *D*, detergent-insoluble cytoskeletons were prepared 3 h after microinjection of the affinity-purified rabbit anti-brain spectrin into an EBTr cell. The distribution of the microinjected antibody was visualized in *C* by staining the cells with fluorescein-labeled goat anti-rabbit IgG. The distribution of spectrin in these Triton-cytoskeletons was visualized in *D* by staining the cells with the monoclonal antibody PHM61 followed by rhodamine-conjugated goat anti-mouse IgG antibody. Bar, 30 μm.

long as the antibody had not caused the spectrin to aggregate (Fig. 6, *A–B*). During early times after microinjection the antibody appeared diffusely distributed all around the cell (Fig. 6*A*). As soon as the nonerythrocyte spectrin was precipitated (~1 h after injection with monoclonal antibody PHM61, not shown), as indicated by the appearance of bright fluorescent patches of aggregated material in the cell, the distribution of the vimentin intermediate filaments became abnormal in most of the injected cells. This effect persisted in some cells up to 2 d after microinjection as did the aggregation of the spectrin. The same effect on these intermediate filaments was observed both with the monoclonal and affinity-purified polyclonal antibodies.

In most cases, following microinjection of nonerythrocyte spectrin antibodies, the vimentin filaments were distorted not at random but rather seemed concentrated in regions coincident with the aggregates of spectrin (Fig. 5, *G–H*, 6, *C–D*). To explore this point further a series of cells microinjected with affinity-purified rabbit anti-bovine brain spectrin antibody were examined for the distribution of intermediate filaments by indirect double-label immunofluorescence microscopy. Double exposure micrographs of the fluorescein fluorescence (aggregated nonerythrocyte spectrin) and rhodamine fluorescence (intermediate filament distribution) were made (Fig. 7). In several areas of the injected cells, patches of aggregated material could be seen to be coincident with concentrations

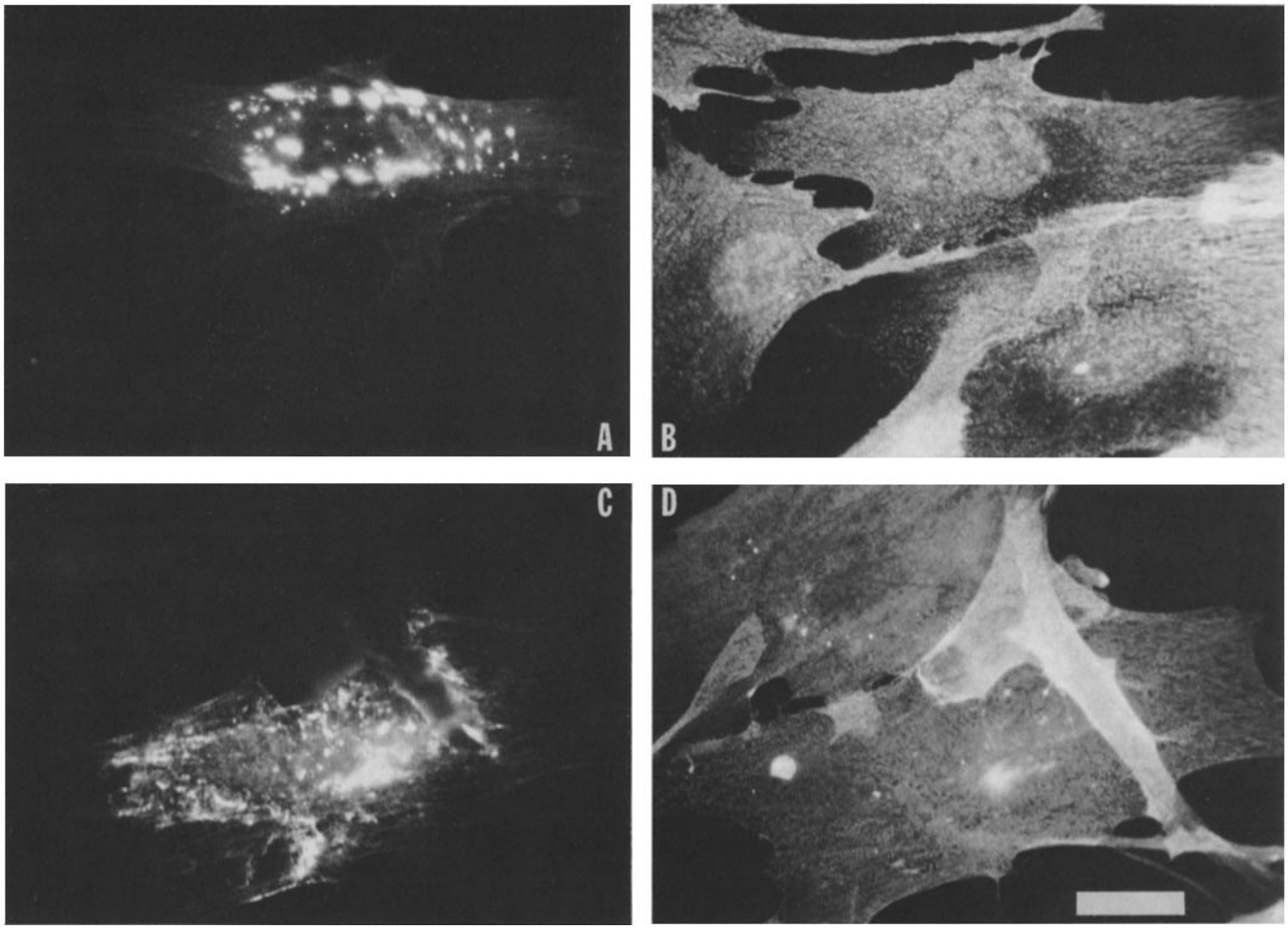

FIGURE 4 The selective precipitation of spectrin within EBTr cells. EBTr cells were microinjected either with affinity-purified rabbit anti-brain spectrin (*A*) or with monoclonal antibody PHM61 (*C*), and 3 h later were fixed and stained with two antibodies giving immunofluorescence patterns similar to the distribution of spectrin (*B* and *D*). (*A* and *B*) Cells were stained with monoclonal antibody PHM526 and then with fluorescein goat anti-rabbit IgG to reveal the microinjected cell (*A*) and rhodamine goat anti-mouse IgG to reveal the distribution of the antigen recognized by PHM526 (*B*). In *C* and *D*, cells were stained with rabbit anti-36-kd protein followed by rhodamine goat anti-mouse IgG to reveal the injected cell (*C*) and fluorescein goat anti-rabbit IgG to reveal the distribution of the 36-kd protein (*D*). Bar, 30 μm.

of intermediate filaments. This coincidence, however, is not complete and regions were apparent where coincidence was not seen or was only minor.

Distortion of Intermediate Filaments Is Specific for Microinjection of Antinonerythrocyte Spectrin Antibodies

The early time-points in the time course experiment indicated that the distortion of intermediate filaments was not the immediate result of a mechanical perturbation during the microinjection procedure. As a further control, cells were microinjected with other antibodies and reagents. No effect on the pattern of intermediate filaments was observed when EBTr cells were microinjected with rhodamine-labeled goat anti-mouse IgG antibodies (Fig. 8, *A–B*). Similarly, the microinjection of rhodamine-labeled vinculin did not distort the intermediate filaments (data not shown). When the monoclonal antibody, PHM61, was injected into cells with which it did not cross-react, such as the gerbil fibroma cells, no effect was seen on the distribution of intermediate filaments. However, the intermediate filaments in these same cells were distorted when the affinity-purified, polyclonal antibody against spectrin was injected into these cells (Fig. 8, *C–F*).

Precipitation of Spectrin within Various Cell Types

Various cell types from different species have been microinjected with the antispectrin antibodies. The monoclonal PHM61 has a more narrow species specificity than the polyclonal rabbit antibody and this latter has been used more extensively. In all cell types examined so far, in which this polyclonal antibody cross-reacts with the spectrin, it has been found to cause spectrin aggregation following microinjection into the cells. The pattern of aggregation, however, varied between cells and in some such as gerbil fibroma and MDBK the aggregates were quickly incorporated into phase-dense, vesicular structures around the nucleus that were probably lysosomes. In most cell types, the aggregation of the spectrin resulted in a distortion of the intermediate filaments as described above. In Hela cells, the intermediate filaments were

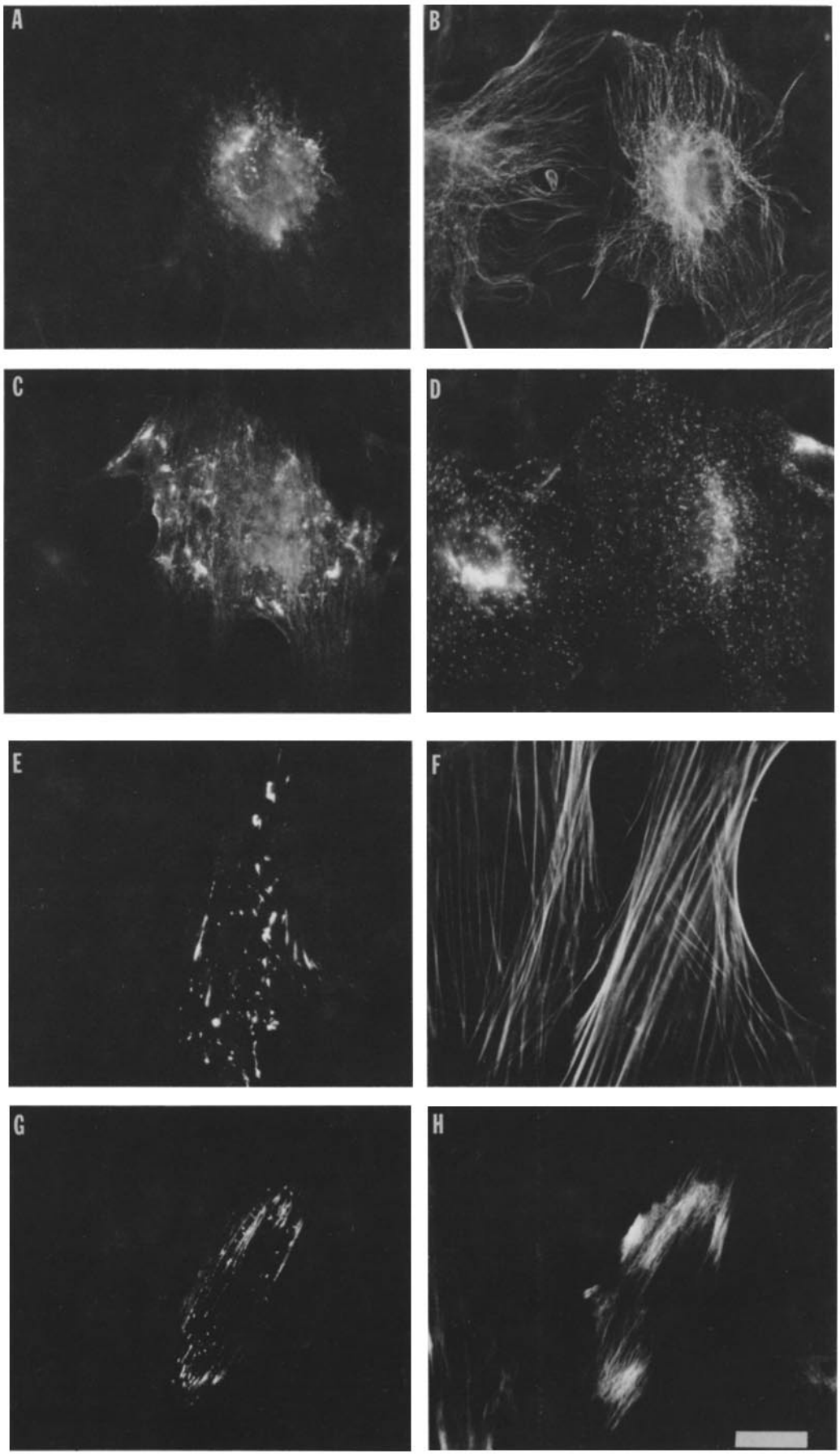

FIGURE 5 Effect of microinjection of nonerythrocyte spectrin antibodies on cytoskeletal structures in EBTr cells. Cells were microinjected with either PHM61 monoclonal antibody (*A–D*) or affinity-purified rabbit anti-bovine brain spectrin (*E–H*) then fixed and premeabilized at 3 h (*A* and *B*), 3 h 30 min (*C* and *D*), 4 h (*E* and *F*), 5 h (*G* and *H*) after microinjection. To reveal the distribution of other cytoskeletal structures, the cells were stained with guinea pig antitubulin (*B*), rabbit anticoated vesicles (*D*), NBD-phallacidin (*F*), or mouse anti-intermediate filaments (JLB7 monoclonal) (*H*), and followed by the appropriate fluorescein- or rhodamine-conjugated second antibodies. Bar, 30 μm.

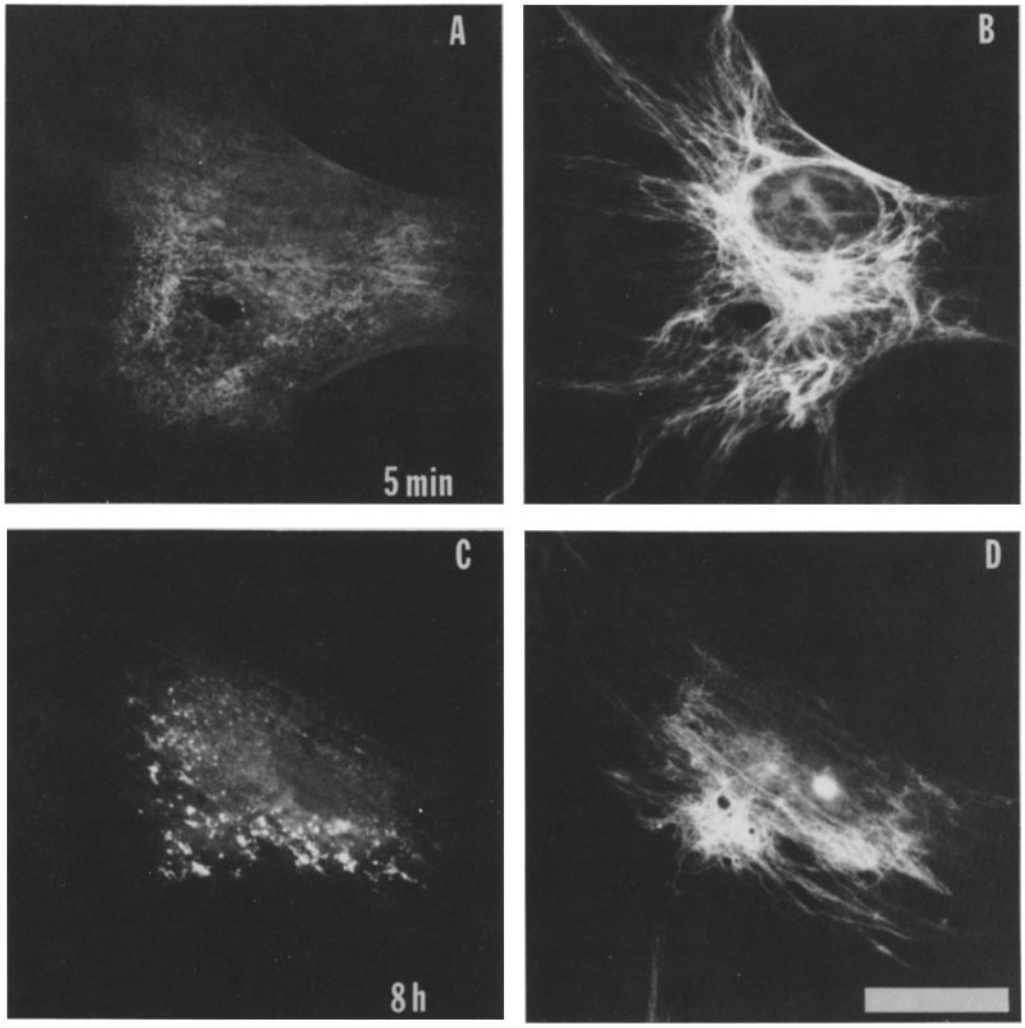

FIGURE 6 Early and late effects of microinjection of monoclonal antibody PHM61 on the distribution of intermediate filaments in EBTr cells. Cells were fixed and permeabilized at the different times indicated after microinjection. Cells were then incubated with an autoimmune rabbit antivimentin filament antibody (*B* and *D*), followed by fluorescein-conjugated goat anti-rabbit IgG antibody and rhodamine-conjugated goat anti-mouse IgG antibody. (*A* and *C*) Micrographs of injected cells selectively viewed with rhodamine optics; (*B* and *D*) micrographs of the same fields selectively viewed for fluorescein fluorescence to allow visualization of the distribution of intermediate filaments. Bar, 30 μm.

caused to concentrate around the nucleus in close correspondence to the aggregated spectrin (Fig. 9, *D–F*).

Some cells underwent mitosis between the time of microinjecting the antispectrin and fixation for subsequent immunofluorescence. An example was seen in Fig. 9 (*A–C*) where two gerbil fibroma daughter cells were separating following division. It is interesting to note that both contained aggregated spectrin, closely associated with the intermediate filaments, which still appeared to link the two cells.

One cell type in which spectrin aggregation appeared to have little effect on the distribution of intermediate filaments was the epithelial cell line MDBK. This was chosen as an example of a polarized epithelial cell where immunofluorescence demonstrated the prominent distribution of spectrin along the epithelial cell border. Microinjection of either the polyclonal or monoclonal antibodies against spectrin resulted in the rapid aggregation of the spectrin in these cells, followed by its apparent internalization into lysosomes within 3 h. At this time the vimentin class of intermediate filaments within these cells appeared essentially normal (Fig. 9, *G–I*). It should be noted that the cells in Fig. 9, *F* and *I* were stained after fixation with the same affinity-purified anti-brain spectrin that was injected, so as to allow visualization of the normal spectrin distribution in uninjected cells as well as to demonstrate that in the injected cells all the detectable spectrin had been precipitated and concentrated into a few compact aggregates.

Microinjection of Colcemid-treated Cells

To study further the relationship between the vimentin intermediate filaments and nonerythrocyte spectrin, EBTr cells were treated with 1 or 10 μM colcemid (both concentrations gave identical results) for 36 h. At this point microtubules are not only disrupted, but intermediate filaments are caused to condense as coils around the nucleus (17, 19). Such colcemid-treated EBTr cells appeared more rounded than nontreated cells and the distribution of the spectrin was more concentrated in the center of the cell over the coiled intermediate filaments, although a faint distribution persisted to

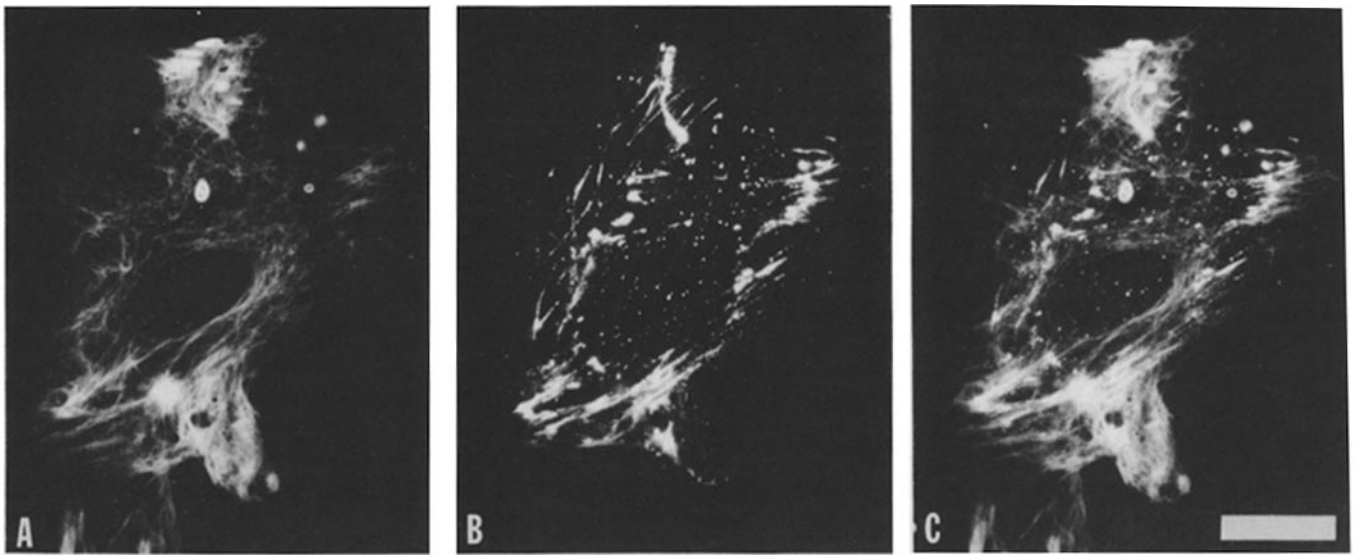

FIGURE 7 Comparison of the distribution of intermediate filaments and spectrin aggregates in microinjected cells. EBTr cells were microinjected with affinity-purified rabbit anti-brain spectrin and 4 h later, fixed, permeabilized, and stained with a mouse monoclonal anti-intermediate filament antibody. *A* shows the distribution of intermediate filaments in the injected cells, whereas *B* shows the aggregated spectrin in the same cells. *C* shows the two distributions superimposed by double exposure of the original negatives. Bar, 30 μm.

the cell margins (Fig. 10, *A–C*). Similar results were reported by Lehto and Virtanen (30). When colcemid-treated cells were microinjected with the affinity-purified, polyclonal antibody against spectrin, bright patches of aggregated spectrin were seen 90 min after microinjection overlying the coiled intermediate filaments (Fig. 10, *D–I*) but some aggregates were also seen in the cell periphery away from the coiled filaments. These peripheral aggregates of spectrin provide evidence against a strong association between the nonerythrocyte spectrin and the vimentin filaments since a clear separation of these aggregates had occurred under these circumstances. These peripheral spectrin aggregates showed a more pronounced linear distribution, co-aligning with the stress fibers seen in the corresponding phase contrast micrograph.

DISCUSSION

We have shown here that nonerythrocyte spectrin can be caused to aggregate within living cells by microinjecting specific antibodies. This same effect has been obtained using either a monoclonal antibody (PHM61) which is an IgM directed against the nonerythrocyte spectrin α chain, or an affinity-purified polyclonal antibody prepared against brain spectrin (fodrin). Comparing the two types of antibody, the polyclonal caused more compact aggregates of spectrin which were also more clearly aligned with stress fibers, whereas the aggregates of spectrin resulting from the microinjection of the monoclonal antibody were less concentrated and more randomly distributed in the cell. This difference probably results from the fact that the monoclonal should interact with only a single site per α chain (or twice per $\alpha_2\beta_2$ tetramer; 15) whereas the polyclonal antibody should bind at multiple sites on both α and β chains with consequently greater affinity for the molecule and more efficient immunoprecipitating properties. Regardless of the nature of the antibody, the important point is that the spectrin within the cell can be quantitatively (as judged by immunofluorescence) and selectively precipitated by microinjection of a specific antibody. Since the spectrin can be precipitated by microinjection such cells become phenotypically equivalent to mutants defective in their nonerythrocyte spectrin until new spectrin has been synthesized. Such cells should be valuable in determining the function of nonerythrocyte spectrin.

As a first step towards establishing the function of nonerythrocyte spectrin we have asked how this intracellular precipitation of the spectrin affects other cytoskeletal structures. That microtubules and coated vesicles remained apparently unaffected (Fig. 5) by the immunoprecipitation of the spectrin within the cell seems a priori not surprising. More interesting is that no effect was observed on the bundles of microfilaments (stress fibers) (Fig. 5). Although the distribution of nonerythrocyte spectrin in fibroblasts shows some avoidance of stress fibers (6, 31), paradoxically the F-actin-binding properties of the protein (2, 6, 7, 12, 24, 31, 41) and its general similarity to erythrocyte spectrin suggest a role in actin-membrane attachment. From our data here, we conclude that if lateral associations between microfilament bundles and the plasma membrane involve spectrin they are not required for the integrity of these bundles, and that membrane anchorage of the microfilament bundles at their ends (not mediated through spectrin) is certainly the predominent factor stabilizing these structures. Attachment of the microfilament bundles more probably involves proteins concentrated in adhesion plaques such as vinculin (5, 10) or talin (4). It should be noted that the adhesion plaques (focal contacts) also appeared unaffected by this aggregation of spectrin (see Fig. 3*A*). Although the integrity of the microfilament bundles remained intact following this precipitation of spectrin, these aggregates often formed or collected along the microfilament bundles. This was particularly prominent when the affinity-purified polyclonal antibody was used to aggregate the spectrin. Why the precipitated spectrin should align with the stress fibers is not clear, but it may indicate some link between these structures and spectrin, however, one that is not essential for the

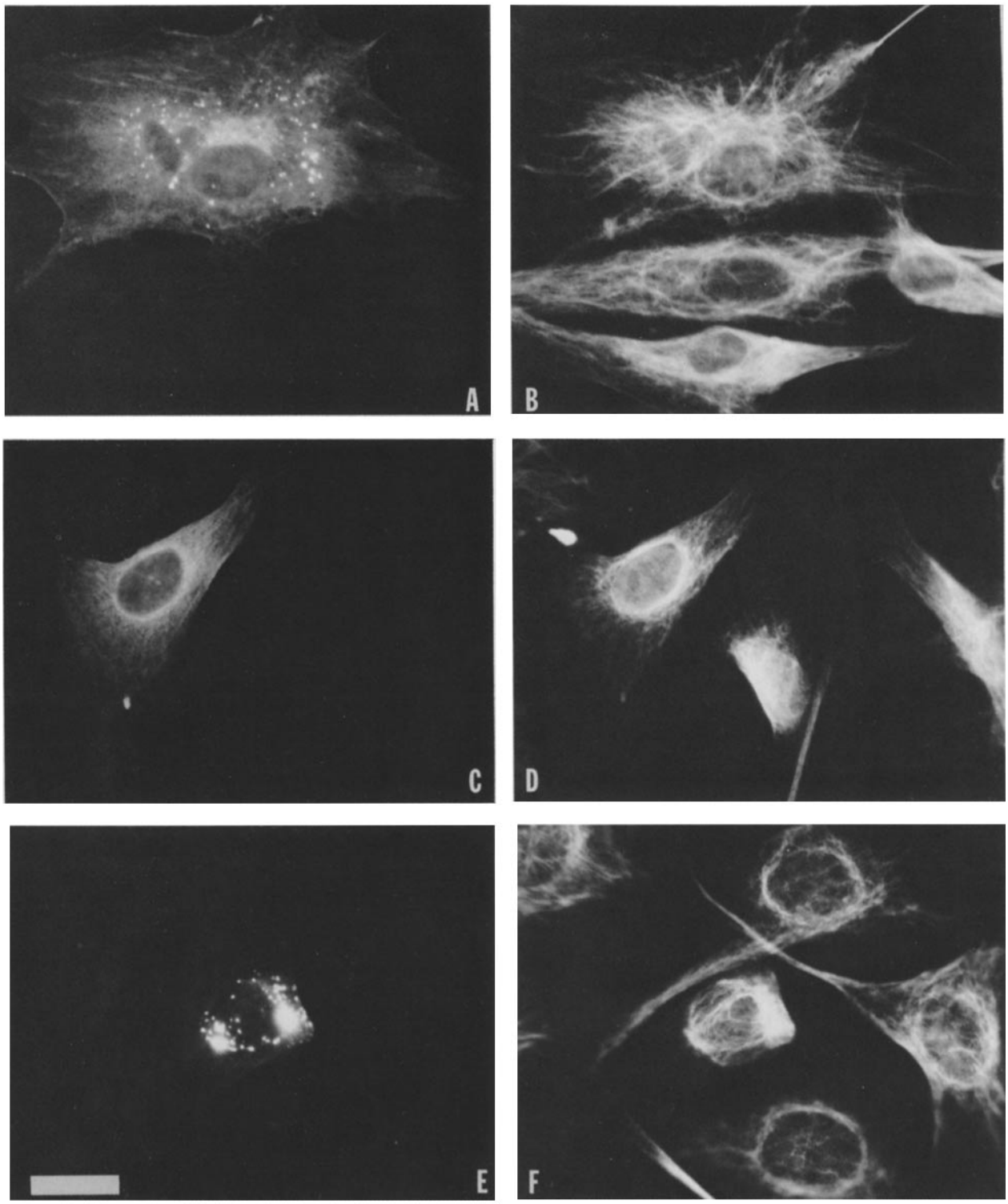

FIGURE 8 The distortion of intermediate filaments is specific for cells injected with precipitating antispectrin antibodies. *A* and *B* show EBTr cells that were injected with rhodamine goat anti-mouse IgG (*A*) and stained for intermediate filaments (*B*). The distribution of intermediate filaments appeared normal in the injected cell in *B*. *C* and *E* show gerbil fibroma cells injected with the monoclonal antibody PHM61 (C) or the polyclonal rabbit anti-brain spectrin (*E*). The monoclonal PHM61 does not recognize the gerbil fibroma spectrin and no precipitation is seen. The corresponding distribution of intermediate filaments is shown in *D* and *F* and appeared unaffected in *D* but somewhat distorted in *F*. Bar, 30 μm.

integrity of the stress fibers. That the microfilament bundles were unaffected by this spectrin precipitation does not imply that the nonerythrocyte spectrin has no function in actin-membrane attachment. Undoubtedly cortical actin, which is associated with the plasma membrane, exists in these cells, although it is difficult to visualize by immunofluorescence microscopy.

The observed redistribution of the vimentin class of intermediate filaments following microinjection of antispectrin was rather unexpected (Fig. 5). The redistribution of these

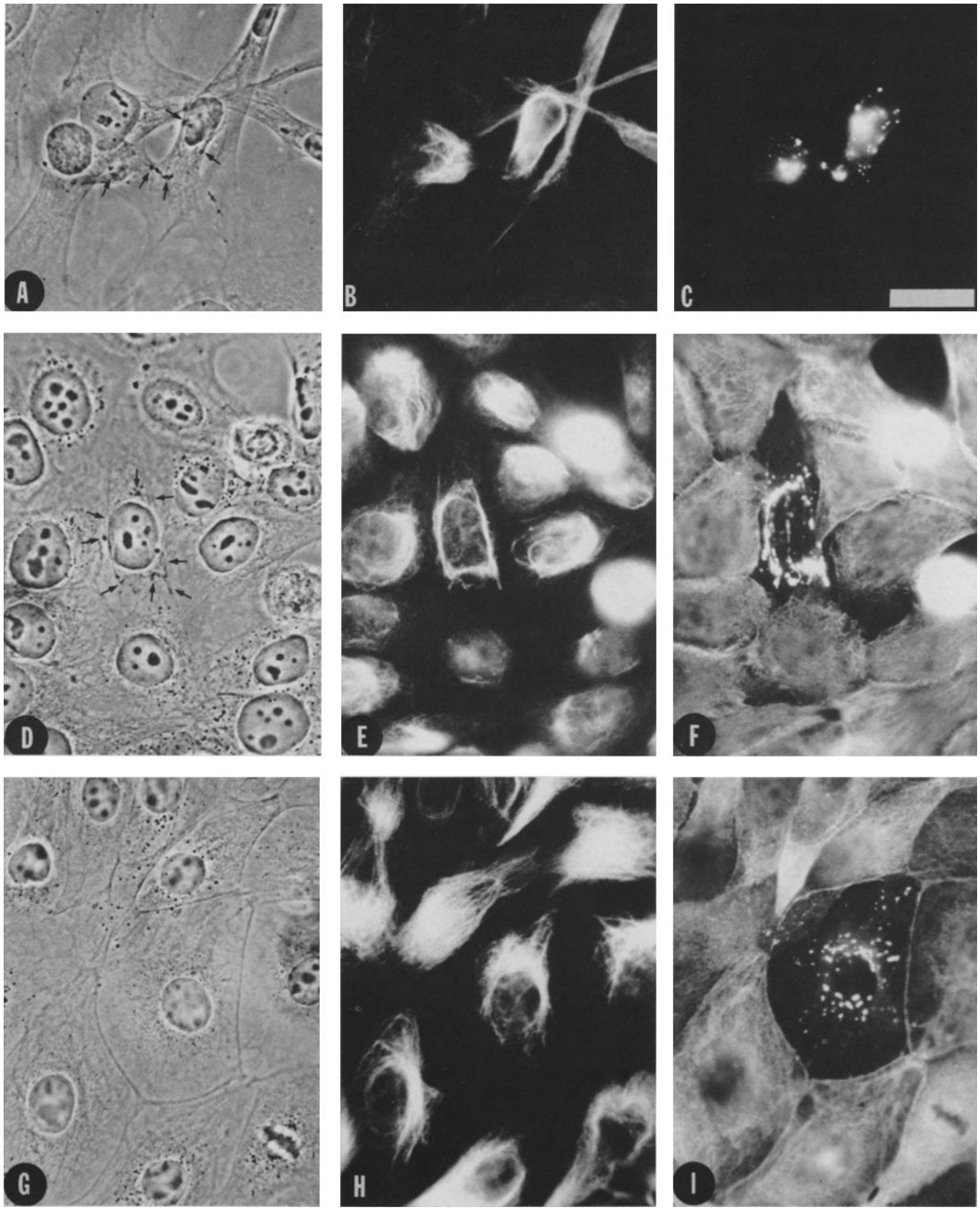

FIGURE 9 Microinjection of anti-brain spectrin into several cell types. Gerbil fibroma cells (*A–C*), Hela cells (*D–F*), and MDBK cells (*G–I*) were microinjected with rabbit anti-brain spectrin 3 h before fixation and processing for indirect immunofluorescence. *A*, *D*, and *G* were phase contrast micrographs. *B*, *E*, and *H* show the same fields, respectively, stained for intermediate filaments. *C* was the same field as in *A* and *B*, but stained to reveal the distribution of the injected antibody. *F* and *I* were the fields corresponding respectively to *D* and *E*, and *G* and *H*, that were stained with the same antispectrin as used in the injections; the microinjected cells were easily recognized by the bright aggregates in contrast to the more diffuse distribution of spectrin in the surrounding, noninjected cells. In *A* and *D*, black arrows point to phase dense precipitated material. Bar, 30 μm.

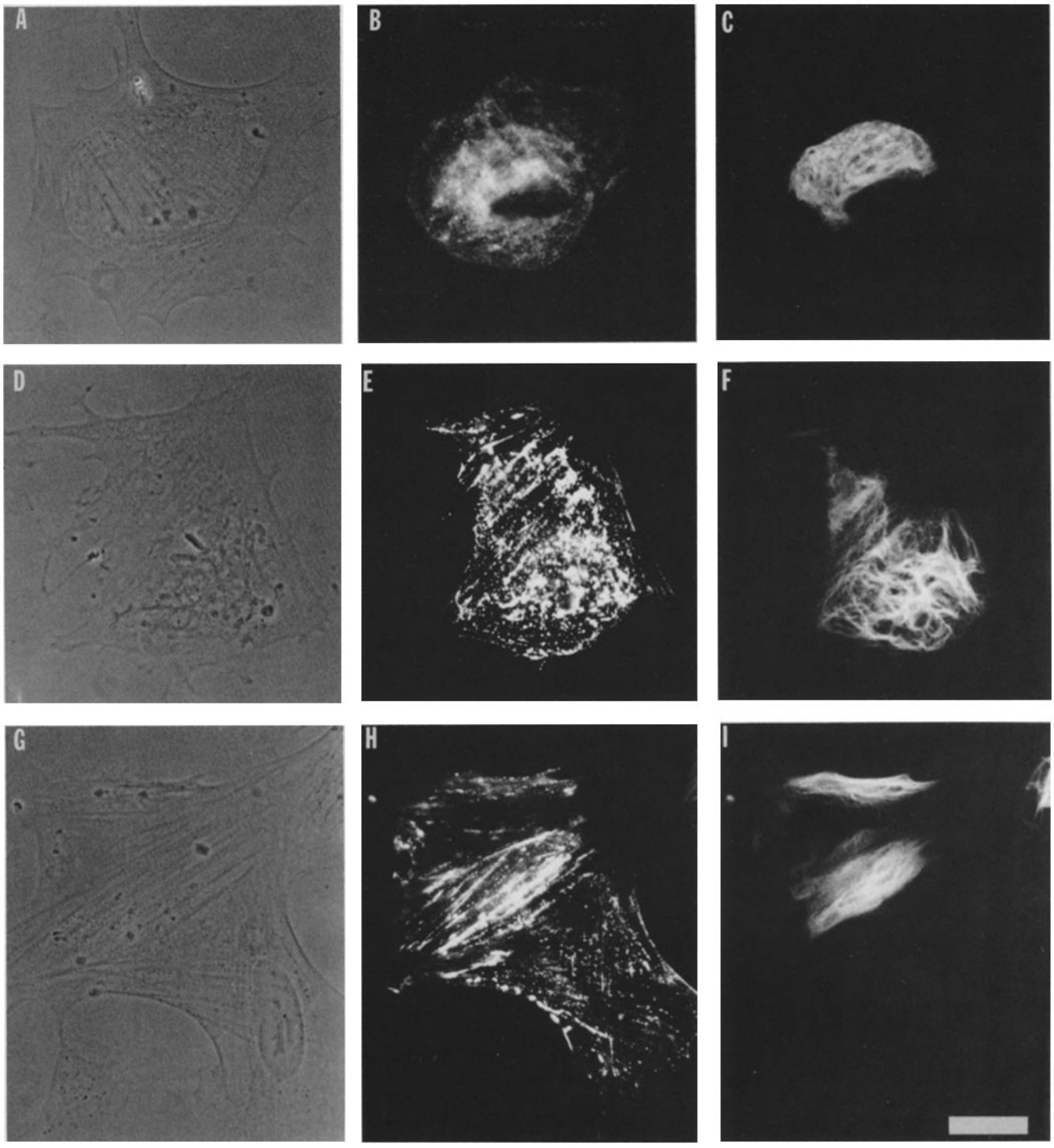

FIGURE 10 Microinjection of nonerythrocyte spectrin antibody into colcemid-treated EBTr cells. Cells were treated with 1 μM colcemid for 36 h then directly fixed, permeabilized, and stained (*A–C*) or microinjected with affinity-purified rabbit anti-bovine brain spectrin antibody 1 h 30 min prior to fixation (*D–I*). Cells were then incubated with a mouse anti-intermediate filament monoclonal antibody (*C, F, I*) alone or together with affinity-purified rabbit anti-bovine brain spectrin (*B*). Fluorescein-conjugated goat anti-rabbit IgG and rhodamine-conjugated goat anti-mouse IgG antibodies were used as second antibodies. *A, D,* and *G* are phase contrast micrographs. *B, E,* and *H* show the same fields viewed under specific fluorescein optics to visualize the spectrin in the cells. *C, F,* and *I* show the same fields viewed under specific rhodamine optics to reveal the distribution of intermediate filaments. Bar, 30 μm.

intermediate filaments was not a total collapse or coiling up as seen with colcemid or upon microinjection of specific antibodies against intermediate filaments (27, 34), but rather it was a more subtle change with the filaments becoming more clumped together and often concentrated in regions where the spectrin could also be seen to have aggregated. This distortion of the vimentin pattern was not seen after microinjection of rhodamine-labeled goat anti-mouse IgG antibodies (Fig. 8) or after injection of rhodamine-labeled vinculin (data not shown) but was found with both monoclonal and poly-

clonal antibodies against spectrin injected into EBTr cells. Only the polyclonal antibody affected the vimentin filaments when injected into gerbil fibroma cells where PHM61 did not cross-react with the spectrin (Fig. 8). The distortion of the vimentin filaments was time-dependent and appeared to correlate with the aggregation of the spectrin (Fig. 6).

One of the few cell types in which little effect of spectrin precipitation was seen on the vimentin intermediate filament pattern was the epithelial cell line MDBK. This may have been due to the extensive network of cytokeratin intermediate filaments within these cells which acted to stabilize the vimentin filaments or, alternatively, this may have been due to the rapid clearance of the spectrin aggregates into presumptive lysosomes within the cells. The rate at which the precipitated spectrin entered presumptive lysosomes varied considerably with the different cell types examined. It was slowest in cells such as EBTr, which had large stress fibers and was fastest in MDBK cells, which had no stress fibers.

Two possible explanations can be suggested for the observed effects on the vimentin filaments. It could be that the system of vimentin filaments is involved in the clearance of precipitated or aggregated material within cells. Arguing against this possibility is the observation that in cells where the precipitated spectrin was most rapidly cleared (as in the MDBK cells) the least distortion of the vimentin filaments was seen. Nevertheless we are currently investigating this possibility further and are looking for other antibodies that cause specific antigens to precipitate within cells. An alternative possibility, which we favor, is that the ends of the vimentin class of intermediate filaments may be linked to the membrane either directly or indirectly via the nonerythrocyte spectrin. As a result of the aggregation of the spectrin the intermediate filaments might also be caused to aggregate within the cell resulting in the distorted pattern and the tendency for the intermediate filaments to align partially with the spectrin aggregates. This possibility is favored by the concentration of spectrin in nonmicroinjected cells in regions overlying coils of vimentin filaments induced by colcemid treatment (Fig. 10, *A–C*). Lehto and Virtanen reported a similar redistribution of a spectrin-related protein in response to colcemid (30). Hirokawa et al. (22) have also demonstrated an association between the spectrin-like molecule, TW260/240 (12) and intermediate filaments present in the terminal web of the brush border of the intestinal epithelium using electron microscopy and specific antibodies. From their electron micrographs, they suggested that the spectrin-like molecules in this system may mediate not only actin-intermediate filament linkages, but actin-vesicle and vesicle-plasma membrane linkages as well. The relationship between intermediate filaments and nonerythrocyte spectrin that we have observed is not absolute. Areas of aggregated spectrin can be seen in microinjected cells which do not correlate with intermediate filaments (Fig. 7) and this is particularly true in colcemid-treated cells (Fig. 10). Here one can find regions of the cell from which the intermediate filaments have been cleared but in which precipitates of nonerythrocyte spectrin are still present.

An interesting issue not raised in this study is what happens to the calmodulin distribution in spectrin-aggregated cells. As nonerythrocyte spectrin is a major calmodulin-binding protein (7, 12, 24) and because of its submembranous localization in the cell, one may speculate that spectrin might be involved in the mediation of Ca^{++}-calmodulin regulatory events triggered by external signals. In this respect, the use of microinjection of antispectrin antibodies into living cells might provide a clue to the significance of the still unexplained calmodulin-binding site on nonerythrocyte spectrin molecules.

The characteristic shape of mammalian erythrocytes is often attributed to spectrin. Does nonerythrocyte spectrin also have a role in determining cell shape? Surprisingly, removal of the spectrin by immunoprecipitation after microinjection of specific antibodies did not seem to affect the shape of the injected cell significantly. Although we have not yet performed a detailed, long-term study of cell shape by time-lapse video recording, we have not observed obvious changes in the cell's shape or appearance except for the usual postmicroinjection transitory change in phase contrast. After microinjection of antispectrin, the cells appeared to behave normally; they continued to divide (Fig. 9), continued to move, and also were able to respread normally following a brief EDTA treatment that caused them to round up (P. Mangeat et al., in preparation).

One of the most interesting properties of erythrocyte spectrin is its relationship to transmembrane components and its restriction of their lateral mobility (9, 16). Do nonerythrocyte spectrins restrict the lateral mobility of surface components in other cell types? One possible way to approach this question should be to use the experimental system we have described here in which nonerythrocyte spectrin can be aggregated within a living cell. Likewise it should be possible to use this approach to determine the role of spectrin in the aggregation and movement of surface molecules that occurs in the capping of lymphocytes and other cells and in which nonerythrocyte spectrin has been implicated (32, 36). Experiments so far, however, that have included investigating the effects of spectrin aggregation on antibody-induced redistribution of β-2 microglobulin, on the lateral mobility of certain surface antigens, and on the phagocytosis of latex beads by macrophages have revealed no striking differences between injected and uninjected cells (P. H. Mangeat et al., in preparation).

Finally, the above results lead us to question the prevailing view that nonerythrocyte spectrin is the major structural component in a submembranous cytoskeletal network that is similar to that found in erythrocytes. Additional evidence against this view comes from the selectivity of the precipitation experiments, in which spectrin can be caused to aggregate without affecting other proteins with apparently the same distribution, such as the 36-kd substrate for $pp60^{src}$ kinase (20, 38, 39). If these other proteins are components of the same cortical submembranous network, then it argues that the network can exist without spectrin.

The authors thank Drs. J. Lin, S. Blose, and S. Martin for their generous gifts of antibodies. Special thanks are extended to Dr. P. Saling for teaching P. H. Mangeat the fusion and cloning techniques and to T. Kelly and L. Hertz for providing purified proteins. We thank S. Hester for photographic assistance and the secretaries of the Department of Anatomy for patiently preparing this manuscript.

This work was supported by a grant from National Institutes of Health (GM29860) and from the Muscular Dystrophy Association.

Received for publication 7 September 1983, and in revised form 7 December 1983.

REFERENCES

1. Barak, L. S., R. R. Yocum, E. A. Nothnagel, and W. W. Webb. 1980. Fluorescence staining of the actin cytoskeleton in living cells with 7-nitrobenz-2-oxa-1,3-diazole-

phallacidin. *Proc. Natl. Acad. Sci. USA.* 77:980–984.
2. Bennett, V., J. Davis, and W. E. Fowler, 1982. Brain spectrin, a membrane associated protein related in structure and function to erythrocyte spectrin. *Nature (Lond.).* 299:126–131.
3. Blose, S. H., and A. Bushnell. 1982. Observations on the vimentin ten-nanometer filaments during mitosis in BHK21 cells. *Exp. Cell Res.* 142:57–62.
4. Burridge, K., and L. Connell. 1983. A new protein of adhesion plaques and ruffling membranes. *J. Cell Biol.* 97:359–367.
5. Burridge, K., and J. R. Feramisco. 1980. Microinjection and localization of a 130K protein in living fibroblasts: a relationship to actin and fibronectin. *Cell.* 19:587–595.
6. Burridge, K., T. Kelly, and P. Mangeat. 1982. Nonerythrocyte spectrins: Actin-membrane attachment proteins occurring in many cell types. *J. Cell Biol.* 95:478–486.
7. Davies, P. J. A., and C. B. Klee. 1981. Calmodulin-binding proteins: a high molecular weight calmodulin-binding protein from bovine brain. *Biochemistry International.* 3:203–212.
8. Feramisco, J. R., and K. Burridge. 1980. A rapid purification of α-actinin, filamin and a 130,000-dalton protein from smooth muscle. *J. Biol. Chem.* 255:1194–1199.
9. Fowler, V., and V. Bennett. 1978. Association of spectrin with its membrane attachment site restricts lateral mobility of human erythrocyte integral membrane proteins. *J. Supramol. Struct.* 8:215–221.
10. Geiger, B. 1979. A 130K protein from chicken gizzards; its localization at the termini of microfilament bundles in cultured chicken cells. *Cell.* 18:193–205.
11. Giloh, H., and J. W. Sedat. 1982. Fluorescence microscopy: reduced photobleaching of rhodamine and fluorescein protein conjugates by n-propyl gallate. *Science (Wash. DC).* 217:1252–1255.
12. Glenney, J. R., P. Glenney, M. Osborn, and K. Weber. 1982. An F-actin- and calmodulin-binding protein from isolated intestinal brush borders has a morphology related to spectrin. *Cell.* 28:843–854.
13. Glenney, J. R., P. Glenney, and K. Weber. 1982. Erythroid spectrin, brain fodrin, and intestinal brush border proteins (TW-260/240) are related molecules containing a common calmodulin-binding subunit bound to a variant cell type-specific subunit. *Proc. Natl. Acad. Sci. USA.* 79:4002–4005.
14. Glenney, J. R., P. Glenney, and K. Weber. 1982. F-actin-binding and cross-linking properties of porcine brain fodrin, a spectrin-related molecule. *J. Biol. Chem.* 257:9781–9787.
15. Glenney, J. R., Jr., P. Glenney, and K. Weber. 1983. Mapping the fodrin molecule with monoclonal antibodies. A general approach for rod-like multidomain proteins. *J. Mol. Biol.* 167:275–293.
16. Golan, D. E., and W. Veatch. 1980. Lateral mobility of band 3 in the human erythrocyte membrane studied by fluorescence photobleaching recovery: evidence for control by cytoskeletal interactions. *Proc. Natl. Acad. Sci. USA.* 77:2537–2541.
17. Goldman, R. D., and D. M. Knipe. 1972. Functions of cytoplasmic fibers in non-muscle cell motility. *Cold Spring Harbor Symp. Quant. Biol.* 37:523–534.
18. Goodman, S. R., I. S. Zagon, and R. R. Kulikowski. 1981. Identification of a spectrin-like protein in nonerythroid cells. *Proc. Natl. Acad. Sci. USA.* 78:7570–7574.
19. Gordon, W. E., III, A. Bushnell, and K. Burridge. 1978. Characterization of the intermediate (10 nm) filaments of cultured cells using an autoimmune rabbit antiserum. *Cell.* 13:249–261.
20. Greenberg, M. E., and G. M. Edelman. 1983. The 34 kd pp60^{src} substrate is located at the inner face of the plasma membrane. *Cell.* 33:767–779.
21. Graessmann, M., and A. Graessmann. 1976. "Early" simian-virus-40-specific RNA contains information for tumor antigen formation and chromatin replication. *Proc. Natl. Acad. Sci. USA.* 73:366–370.
22. Hirokawa, N., R. E. Cheney, and M. Willard. 1983. Location of a protein of the fodrin-spectrin. TW260/240 family in the mouse intestinal brush border. *Cell.* 32:953–965.
23. Hunter, W. M., and F. C. Greenwood. 1962. Preparation of iodine-131 labeled human growth hormone of high specific activity. *Nature (Lond.).* 194:495–496.
24. Kakiuchi, S., K. Sobue, K. Kanda, K. Morimoto, S. Tsukita, S. Tsukita, H. Ishikawa, and M. Kurokawa. 1982. Correlative biochemical and morphological studies of brain calspectin: a spectrin-like calmodulin-binding protein. *Biomed. Res.* 3:400–410.
25. Keen, J. H., M. C. Willingham, and I. Pastan. 1981. Clathrin and coated vesicles: immunological characterization. *J. Biol. Chem.* 256:2538–2544.
26. Kennett, R. 1979. Cell fusion. *Methods Enzymol.* 58:345–349.
27. Klymkowsky, M. W. L. 1981. Intermediate filaments in 3T3 cells collapse after intracellular injection of a monoclonal anti-intermediate filament antibody. *Nature (Lond.).* 291:249–251.
28. Köhler, G., and C. Milstein. 1975. Continuous cultures of fused cells secreting antibody of predefined specificity. *Nature (Lond.).* 256:495–497.
29. Laemmli, U. K. 1970. Cleavage of structural proteins during the assembly of the head of bacteriophage T4. *Nature (Lond.).* 227:680–685.
30. Lehto, V.-P., and I. Virtanen. 1983. Immunolocalization of a novel, cytoskeleton-associated polypeptide of Mr 230,000 daltons (p 230). *J. Cell Biol.* 96:703–716.
31. Levine, J., and M. Willard. 1981. Fodrin: axonally transported polypeptides associated with the internal periphery of many cells. *J. Cell Biol.* 90:631–643.
32. Levine, J., and M. Willard. 1983. Redistribution of fodrin (a component of the cortical cytoplasm) accompanying capping of cell surface molecules. *Proc. Natl. Acad. Sci. USA.* 80:191–195.
33. Lin, J. J. -C. 1981. Monoclonal antibodies against myofibrillar components of rat skeletal muscle decorate the intermediate filaments of cultured cells. *Proc. Natl. Acad. Sci. USA.* 78:2335–2339.
34. Lin, J. J.-C., and J. R. Feramisco. 1981. Disruption of the in vivo distribution of the intermediate filaments in fibroblasts through the microinjection of a specific monoclonal antibody. *Cell.* 24:185–193.
35. Mangeat, P. H., and K. Burridge. 1983. Binding of Hela spectrin to a specific Hela membrane fraction. *Cell Motility.* 3:657–669.
36. Nelson, W. J., C. A. L. S. Colaco, and E. Lazarides. 1983. Involvement of spectrin in cell-surface receptor capping in lymphocytes. *Proc. Natl. Acad. Sci. USA.* 80:1626–1630.
37. Nelson, W. J., and E. Lazarides. 1983. Expression of the β subunit of spectrin in nonerythroid cells. *Proc. Natl. Acad. Sci. USA.* 80:363–367.
38. Nigg, E. A., J. A. Copper, and T. Hunter. 1983. Immunofluorescent localization of a 39,000-dalton substrate of tyrosine protein kinase to the cytoplasmic surface of the plasma membrane. *J. Cell Biol.* 96:1601–1609.
39. Radke, K., V. C. Carter, P. Moss, P. Dehazya, M. Schliwa, and G. S. Martin. 1983. Membrane association of a 36,000 dalton substrate for tyrosine phosphorylation in chicken embryo fibroblasts transformed by avian sarcoma viruses. *J. Cell Biol.* 97:1601–1611.
40. Repasky, E. G., B. L. Granger, and E. Lazarides. 1982. Widespread occurrence of avian spectrin in non-erythroid cells. *Cell.* 29:821–833.
41. Sobue, K., K. Kanda, M. Inui, K. Morimoto, and S. Kakiuchi. 1982. Actin polymerization induced by calspectin, a calmodulin-binding spectrin-like protein. *FEBS Fed. Eur. Biol. Soc. Lett.* 148:221–225.
42. Ternynck, T., and S. Avrameas. 1972. Polyacrylamide-protein immunoadsorbents prepared with glutaraldehyde. *FEBS Fed. Eur. Biol. Soc. Lett.* 23:24–28.
43. Towbin, H., T. Staehelin, and J. Gordon. 1979. Electrophoretic transfer of proteins from polyacrylamide gels to nitrocellulose sheets; procedure and some applications. *Proc. Natl. Acad. Sci. USA.* 76:4350–4354.